Advanced Pharmaceutical Bulletin

Accepted Manuscript (unedited)

The manuscript will undergo copyediting, typesetting, and review of the resulting proof before it is published in its final form.

Research Article

How to cite this article:
Yazdani Z, Sohbatzadeh F, Abediankenari S, Golpour M, Fattahi S, Rafiei A. Redox-Mediated Sensitization of Melanoma Cells to Vemurafenib by Cold Atmospheric Plasma: A Molecular Insight into Apoptotic and Autophagic Regulation. Advanced Pharmaceutical Bulletin, doi: 10.34172/apb.46838

Redox-Mediated Sensitization of Melanoma Cells to Vemurafenib by Cold Atmospheric Plasma: A Molecular Insight into Apoptotic and Autophagic Regulation

Zahra Yazdani [1, 2], Farshad Sohbatzadeh [3], Saeid Abediankenari [4], Monireh Golpour [1,5], Sadegh Fattahi [6], Alireza Rafiei [1]*

1. Department of Immunology, Molecular and Cell Biology Research Center, School of Medicine, Mazandaran University of Medical Sciences, Sari, Iran.
2. Students Research Committee, Mazandaran University of Medical Sciences, Sari, Iran.
3. Department of Atomic and Molecular Physics, Faculty of Science, University of Mazandaran, Babolsar, Iran.
4. Immunogenetics Research Center, Department of Immunology, Faculty of Medicine, Mazandaran University of Medical Sciences, Sari, Iran.
5. Cancer Research Center, Health Research Institute, Babol University of Medical Sciences, Babol, Iran.
6. North Research Center of Pasteur Institute, Amol, Iran.

ARTICLE INFO

Keywords:
Cold atmospheric plasma,
Vemurafenib,
Melanoma,
Reactive oxygen species,
Apoptosis,
Autophagy

Article History:
Submitted: December 02, 2025
Revised: June 17, 2026
Accepted: June 29, 2026
ePublished: July 12, 2026

ABSTRACT

Purpose: This study investigated the combined effects of cold atmospheric plasma (CAP) and vemurafenib (VEM) on malignant melanoma, focusing on redox signaling, apoptosis, and autophagy.

Methods: Murine melanoma B16-F10 cells and normal L929 fibroblasts were treated with CAP, VEM, or their combination. Cell viability was assessed using the MTT assay. Reactive oxygen and nitrogen species (RONS) and lipid peroxidation were measured to evaluate oxidative stress. Cell cycle distribution and apoptosis were analyzed by propidium iodide (PI) staining and Annexin V-FITC/PI flow cytometry. An in vivo B16-F10 tumor-bearing mouse model was utilized to evaluate tumor growth and molecular changes in tumor tissues. The expression of apoptosis- and autophagy-related genes (BAX, BCL-2, CASP3, LC3, and ATG5) was quantified by qRT-PCR in vitro and in vivo experiments.

Results: The combination treatment significantly reduced the viability of B16-F10 melanoma cells with minimal effects on L929 fibroblasts. This reduction was associated with increased RONS production and lipid peroxidation. Cell cycle analysis indicated S-phase arrest in melanoma cells, and apoptosis assays showed enhanced apoptotic cell death after the combination treatment. Molecular analysis revealed increased expression of BAX and CASP3, whereas BCL-2 expression showed a decreasing trend. The treatment also increased autophagy-related gene expression. In the mouse melanoma model, the combined therapy suppressed tumor growth and increased the expression of apoptosis- and autophagy-related genes, including BAX, CASP3, ATG5, and LC3.

Conclusion: CAP enhances the antitumor effects of VEM by promoting oxidative stress and activating apoptosis- and autophagy-related gene expression. This combined approach may represent a promising strategy for melanoma treatment, although further studies are needed to confirm these findings.

*** Corresponding Author**
Alireza Rafiei, E-mail: rafiei1710@gmail.com, ORCID: 0000-0002-1766-6605

Introduction

Malignant melanoma is one of the most aggressive types of skin cancer. This malignancy originates from the uncontrolled proliferation of melanocytes.[1,2] Over the past few decades, the global incidence of melanoma has increased. According to global cancer statistics, approximately 325,000 new melanoma cases and 57,000 related deaths were reported worldwide in 2020 across 185 countries. [3] Melanoma cells often exhibit high resistance to conventional therapeutic approaches including chemotherapy, radiotherapy, and certain immunotherapies .[4,5]

Vemurafenib (VEM) is a selective small-molecule inhibitor of BRAF kinase. This drug is approved by the U.S. Food and Drug Administration (FDA) for the treatment of melanoma. [6-8] Although the precise molecular mechanisms underlying its anticancer activity are not fully understood, several studies have suggested that VEM can induce the production of reactive oxygen species (ROS) and activate intrinsic apoptotic pathways. These pathways include cytochrome c release and activation of stress‐related kinases such as JNK and p38 MAPK, ultimately leading to caspase activation and apoptotic cell death. [9-12] Despite its notable clinical efficacy, the therapeutic benefits of VEM are frequently limited by several factors, including the development of drug resistance, systemic toxicity, and dermatological adverse effects in some patients.[13-15] Resistance to VEM represents a major clinical challenge in melanoma treatment. Multiple mechanisms have been implicated in the emergence of resistance, including the reactivation of the MAPK signaling pathway, the activation of compensatory survival pathways such as PI3K/AKT, and enhanced cellular tolerance to oxidative stress. These adaptive responses enable tumor cells to maintain survival signaling and reduce the long‐term effectiveness of BRAF inhibitors. Consequently, therapeutic strategies capable of disrupting redox homeostasis, promoting apoptosis, or targeting additional stress‐related pathways may provide a rational approach to enhance the antitumor efficacy of VEM and potentially mitigate resistance‐associated mechanisms.[10,16]

Cold atmospheric plasma (CAP) is a new strategy that is being rapidly investigated in both oncology and regenerative medicine.[17-20] CAP is an ionized gas composed of reactive oxygen and nitrogen species (RONS), ultraviolet (UV) photons, electrons, and charged particles. The elevated levels of RONS generated by CAP can induce oxidative stress and promote selective cytotoxicity in various cancer cell types, including melanoma, breast cancer, glioblastoma, and leukemia *in vitro*.[21-28] Additionally, it has been shown to reduce the size of solid tumors *in vivo*.[17,29-31] Recent studies suggest that combining CAP with conventional anticancer therapies may enhance therapeutic efficacy through synergistic or additive inhibitory mechanisms.[32-37] CAP‐generated reactive species can disrupt the cellular redox balance, alter membrane permeability, and activate multiple cell‐death pathways, which may sensitize cancer cells to anticancer agents. Given that VEM targets oncogenic signaling pathways while CAP induces oxidative and cellular stress responses, their combination may enhance anticancer activity through complementary mechanisms. Accordingly, the present study aimed to investigate the combined effects of CAP and VEM (CAP+VEM) on melanoma inhibition. Specifically, it evaluated their impact on cell viability, apoptosis, autophagy, and tumor growth using murine melanoma models in both *in vitro* and *in vivo* experimental systems.

Methods

Materials and Reagents

VEM (≥98% purity) was obtained from a commercial supplier. It was dissolved in dimethyl sulfoxide (DMSO) to prepare a 10 mM stock solution, which was aliquoted and stored at -80 °C. RPMI-1640 medium, fetal bovine serum (FBS), penicillin-streptomycin, and trypsin-EDTA were obtained from Biosera (France). The MDA assay kit, and Annexin V-FITC/ propidium iodide (PI) apoptosis detection kit were purchased from Teb Pazhouhan Razi (Iran) and eBioscience (San Diego, CA), respectively. The RNA extraction kit, cDNA synthesis kit, and qPCR reagents were obtained from Favourgene (Taiwan), Addbio (South Korea), and Qiagen (Hilden, Germany), respectively. All other chemicals and reagents were of analytical grade and purchased from Sigma-Aldrich (St. Louis, MO), unless otherwise specified.

Cell culture

The murine melanoma cell line B16-F10 and the normal murine fibroblast cell line L929 were obtained from the Pasteur Institute of Iran (Tehran, Iran). Both cell lines were cultured and grown in RPMI-1640 medium supplemented with 10% FBS and 1% penicillin-streptomycin. The cells were kept in an incubator at 37°C with 5% CO2 and high humidity. The culture medium was changed every three days. When the cells reached 70–80% confluency, subculturing was performed using a 0.25% trypsin-EDTA solution.

Determination of the effective concentrations of VEM and exposure times of CAP in inhibiting cell proliferation

To evaluate the effects of CAP, VEM, and CAP+VEM on cell proliferation, cultured cells were treated with each modality alone as well as in combination. After treatment, the cells were incubated for 24, 48, and 72 hours (h). Untreated wells were used as negative controls. CAP was generated using a plasma jet device composed of a cylindrical copper tube serving as the powered electrode, a grounded copper ring electrode, and a Pyrex tube acting as the dielectric barrier. The electrodes were driven by a high‑voltage power supply operating in the range of 0–25 kV with a frequency of 9 kHz. Argon gas (purity 99.999%) was used as the working gas and delivered through the Pyrex tube at a flow rate of 2.5 standard liters per minute. For cell treatment, the plasma jet nozzle was positioned approximately 3 cm above the surface of the culture medium. Cells were exposed to CAP at an applied voltage of 14 kV for exposure times ranging from 20 to 60 seconds (s).[5,17,38] For the VEM treatment, cells from each cell line were exposed to a concentration range of 1–100 µM. To evaluate CAP+VEM, cells were first treated with the IC_{50} concentration of VEM. Cells were pretreated with VEM for 1 h prior to CAP exposure to allow sufficient cellular uptake of the drug, as previous studies have shown that VEM analogs can penetrate melanoma cells and localize in the cytoplasm within approximately one hour.[39] After 24, 48, and 72 h of incubation, 10 µL of MTT reagent was added to each well. The plates were incubated at 37°C for 4 h to facilitate the formation of formazan crystals. Finally, 100 µL of DMSO was added to each well to dissolve the formazan. The optical density (OD) was measured using a BioTek microplate reader (BioTek, Winooski, VT) at wavelengths of 490-630 nm. [40]

Cell morphology assessment by inverted microscopy

To assess changes associated with cytotoxicity, B16-F10 and L929 cells were observed under an inverted phase-contrast microscope. After treatment with VEM, CAP, or CAP+VEM for 24 h, cells were placed under an inverted microscope (Motic, China). The magnification was 100×. Morphological features including cell shrinkage, membrane blebbing, detachment, and loss of adherence, were recorded as indicators of cytotoxicity and apoptosis.

Intracellular ROS measurement

The fluorescent dye H2DCFDA was used to evaluate the presence of intracellular ROS. B16-F10 and L929 cells were cultured in 24-well plates and treated with CAP, VEM, or their combination. Both cell lines were then trypsinized after 24 h and incubated with H2DCFDA. Catalase and H_2O_2 were used as negative and positive controls, respectively. ROS generation was analyzed using a flow cytometer (Partec GmbH, Görlitz, Germany).[36,40]

Production of nitric oxide (NO)

The Griess reaction was performed to quantify nitrite, a product of NO. Briefly, the standard solution was prepared using deionized water and concentrations of 0, 3.125, 6.253, 12.5, 25, 50, 100, 200, 400, 800, and 1000 µM of $NaNO_2$. Each sample was added in five technical replicates per 96-well microplate. 100 µL of each sample and the standard were added separately. Then, 50 µL of 2% sulfanilamide (in 5% HCl) and 50 µmL of 0.1% N-naphthyl-ethylenediamine were added to each well and incubated for 30 min at 37 °C. The OD of each reaction mixture was measured at 540 nm using a BioTek microplate reader. Linear regression analysis of the standard samples was performed for the quantification of the nitrite concentrations in micromolar.[41]

Determination of lipid peroxidation

Lipid peroxidation was determined by measuring the levels of malondialdehyde (MDA). Briefly, after treatment and incubation of the cells for 24 h, the supernatant was collected. Then, an MDA assay was performed using the MDA assay kit. Finally, MDA levels measured at 540 nm using a microplate reader (BioTek, Winooski, VT).

Cell Cycle Analysis

To evaluate the effects of CAP, VEM, and CAP+VEM on cell cycle progression, a flow cytometric assay was performed using PI staining. B16-F10 and L929 cells were seeded in 24-well plates at a density of 1.2×10^5 cells per well. After overnight incubation, the cells were subjected to the following treatments: CAP exposure (70s), VEM (20 µM), and CAP+VEM. After 24 h of incubation, cells were harvested by trypsinization, washed with cold phosphate-buffered saline (PBS), and fixed in 70% ethanol at +4°C overnight. After that, the cells were washed again with PBS and 0.05% of Triton X-100. Finally, the cells were incubated with 500 µL of PI staining solution containing 20 µg/mL PI and 40 µg/mL RNase A for 30 minutes at room temperature in the dark. DNA content was then analyzed using a flow cytometer. Cell cycle distribution (G1, S, and G2/M phases) was determined using FlowJo software.[42]

Annexin V-FITC/PI and PI staining

Apoptotic cell death was determined by flow cytometry and staining with the Annexin V-FITC/PI kit. Cells were incubated in 24 well plates following the treatments and washed with PBS. The apoptosis assay was performed using the Annexin V-FITC/PI staining kit followed by the analysis of cell apoptosis using a flow cytometer and FlowJo software v_10.10.0.

Animal model and treatment

Female C57BL/6 mice (6–8 weeks old; total n = 25) were utilized to develop a murine melanoma model. Each animal received a subcutaneous injection of B16‑F10 melanoma cells (8.5×10^5 cells suspended in 100 µL of

PBS into the right flank. Tumor development was observed daily. Therapeutic interventions were initiated when tumors became palpable (~7 days after cell inoculation). The animals were then randomly allocated into four groups of untreated, VEM, CAP, and CAP+VEM. For plasma treatment, mice were anesthetized using a ketamine–xylazine mixture. The CAP jet was directed toward the tumor with the nozzle positioned about 3 cm above the tumor surface, and exposure was applied for 5 minutes. VEM was administered orally by gavage at a daily dose of 70 mg/kg. Animals were monitored throughout the experiment for tumor progression, body weight, and general health status. Fourteen days after treatment initiation, the mice were sacrificed. Humane endpoints were defined as more than 15% loss of initial body weight, noticeable deterioration in physical condition, or the appearance of severe disease‐related signs. At the conclusion of the study, tumors were excised for the gene expression assay. All animal procedures were carried out following institutional ethical guidelines and were approved by the Research Ethics Committee of Mazandaran University of Medical Sciences (approval code: IR.MAZUMS.AEC.1402.079).

RNA extraction and quantitative real-time PCR (qPCR) using TaqMan probes

For the *in vitro* experiments, total RNA was extracted from B16-F10 and L929 cells using an RNA extraction kit following the manufacturer's instructions and repeated in triplicate. For the *in vivo* analysis, approximately 50 mg of each snap‐frozen tumor tissue was mechanically homogenized, and total RNA was subsequently isolated using a commercial RNA extraction kit following the manufacturer's protocol. For both *in vitro* and *in vivo* samples, about 80 nanograms of total RNA was reverse-transcribed to complementary DNA (cDNA) using the cDNA Reverse Transcription Kit, according to the manufacturer's protocol. The qPCR was performed using TaqMan gene expression assays as described by Fattahi et al [42,43]. The following thermal cycling conditions were used: initial denaturation at 95 °C for 15 minutes, followed by 45 cycles of 95 °C for 15s and 60 °C for 60s. The gene expression of BAX, BCL-2, Caspase 3 (CASP3), LC3, and ATG5 was normalized to the GAPDH reference gene. Relative gene expression levels were determined using the $2^{\wedge-\Delta\Delta Ct}$ method. The data were analyzed using StepOne Software v2.3 (Applied Biosystems).

Use of Artificial Intelligence Tools

During the preparation of this manuscript, the authors used ChatGPT (OpenAI, San Francisco, CA, USA) to assist with language editing and to improve the clarity and readability of the text. The tool was also used to help draft the schematic illustration presented in the graphical abstract, based on the authors' conceptual design and scientific interpretation. The artificial intelligence tool was not used to generate scientific data, perform data analysis, or independently interpret the results. All experimental data, analyses, interpretations, and conclusions were developed and verified by the authors, who take full responsibility for the accuracy and integrity of the work.

Results

VEM exhibits selective and dose‐dependent cytotoxicity in melanoma cells

To evaluate the dose-dependent cytotoxicity of VEM, B16-F10 melanoma cells and L929 normal fibroblasts were treated with increasing concentrations of VEM (0–1000 μM). The MTT assay was employed to assess cell viability after 24 h. This assay allowed for the measurement of the effect of various VEM concentrations on cell proliferation. The resulting data were plotted using GraphPad Prism 8 and analyzed by SPSS 22 (Figure 1). The results showed that treatment with 12 μM VEM reduced cell viability to approximately 72%, while 25 μM of it

decreased viability to about 33% compared with untreated controls (P<0.0001). At 50 µM, VEM induced near-complete cytotoxicity in B16‑F10 cells, reducing viability to less than 5% (P<0.0001). In contrast, L929 fibroblasts exhibited markedly lower sensitivity to VEM. Even at 25 µM, cell viability remained above 85–90%, and at 50 µM approximately 75–80% of cells remained viable, indicating selective cytotoxicity toward melanoma cells. The IC_{50} values obtained from the dose–response curves indicated a marked difference in sensitivity between melanoma and normal fibroblast cells. The IC_{50} value for VEM in B16‑F10 cells was 18 µM, whereas the IC_{50} for L929 cells was 87 µM. Based on these values, the selectivity index (SI = IC_{50} normal / IC_{50} cancer) was calculated to be 4.833, indicating preferential cytotoxicity toward melanoma cells. Based on the IC50 values, a concentration of 20µM was selected for subsequent combination treatment experiments involving CAP+ VEM using the MTT assay.

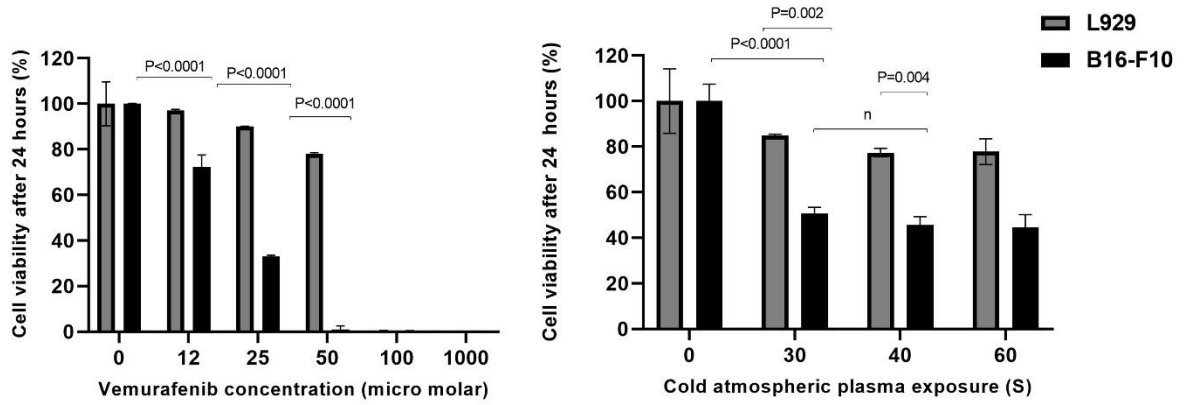

Figure 1. Cytotoxic effects of (A) vemurafenib, and (B) cold atmospheric plasma on B16-F10 melanoma cancer and L929 fibroblast cell lines evaluated by MTT assay 24 hours after treatment.

CAP selectively reduces melanoma cell viability

To investigate the cytotoxic effect of CAP, B16-F10 melanoma cells and L929 normal fibroblasts were exposed during varies time. While other conditions, such as apparatus voltage and distance from nozzle to the sample, were kept constant. Following a 24 h incubation period, cell viability was measured using the MTT assay. This step aimed to evaluate the selective cytotoxicity of CAP and its potential differential effect on cancerous versus normal cell lines, which serves as a basis for its use in combination therapy with VEM. The results showed CAP exposure for up to 30s reduced B16‑F10 viability to approximately 50% (P<0.0001), whereas 40s and 60s exposures decreased viability to around 45% and 43%, respectively (P=0.004). In contrast, L929 fibroblasts displayed minimal sensitivity to CAP treatment, maintaining cell viability above 75–85% across all exposure times, with no statistically significant cytotoxic effects observed. These findings demonstrate the selective cytotoxicity of CAP toward melanoma cells. Based on these results, CAP exposure times of 30s and 40s were selected for subsequent combination treatment experiments with VEM.

CAP+VEM treatment enhances growth inhibition in melanoma cells

To evaluate the potential for enhanced therapeutic efficacy, B16‑F10 melanoma cells and L929 fibroblasts were treated with CAP (30 and 45s), VEM (20 µM), or CAP+VEM, and cell viability was assessed at 24, 48, and 72 h (Figure 2). Statistical analysis confirmed that both CAP and VEM as monotherapies significantly reduced B16‑F10 viability across all time points (P<0.0001). As shown in Figure 2A, fallowing 24 h, VEM monotherapy

reduced B16‑F10 viability to approximately 38%, while 30s and 45s CAP exposure resulted in 52% and 43% viability, respectively. CAP+VEM significantly outperformed monotherapies, further reducing melanoma viability to 22% (CAP 30s + VEM) and 19% (CAP 45s +VEM) (P<0.0001 vs. monotherapy). In contrast, L929 cells remained significantly more viable, with the CAP+VEM treatments maintaining approximately 52% and 43% viability, respectively, indicating a higher sensitivity of cancer cells to the co-treatment. The most pronounced inhibitory effects were observed at 48 h (Figure 2B). In B16‑F10 cells, CAP+VEM led to a near-complete suppression of cell growth, with viability dropping to approximately 12% (CAP 30s+VEM) and 9% (CAP 45s+VEM), which was significantly lower than VEM alone (25%) or CAP alone (45%). Although CAP+VEM also reduced L929 viability at this time point (to ~30–33%), the survival rate of normal fibroblasts was still 3-fold higher than that of the melanoma cells, highlighting the therapeutic window of the combination. At 72 h (Figure 2C), while B16-F10 cells treated with VEM alone showed a relative increase in viability (reaching ~56%), CAP+VEM treated cells remained suppressed at approximately 20% (CAP 30s + VEM) and 18% (CAP 45s+VEM). This suggests that the addition of CAP provides a more sustained inhibitory effect compared to VEM monotherapy.

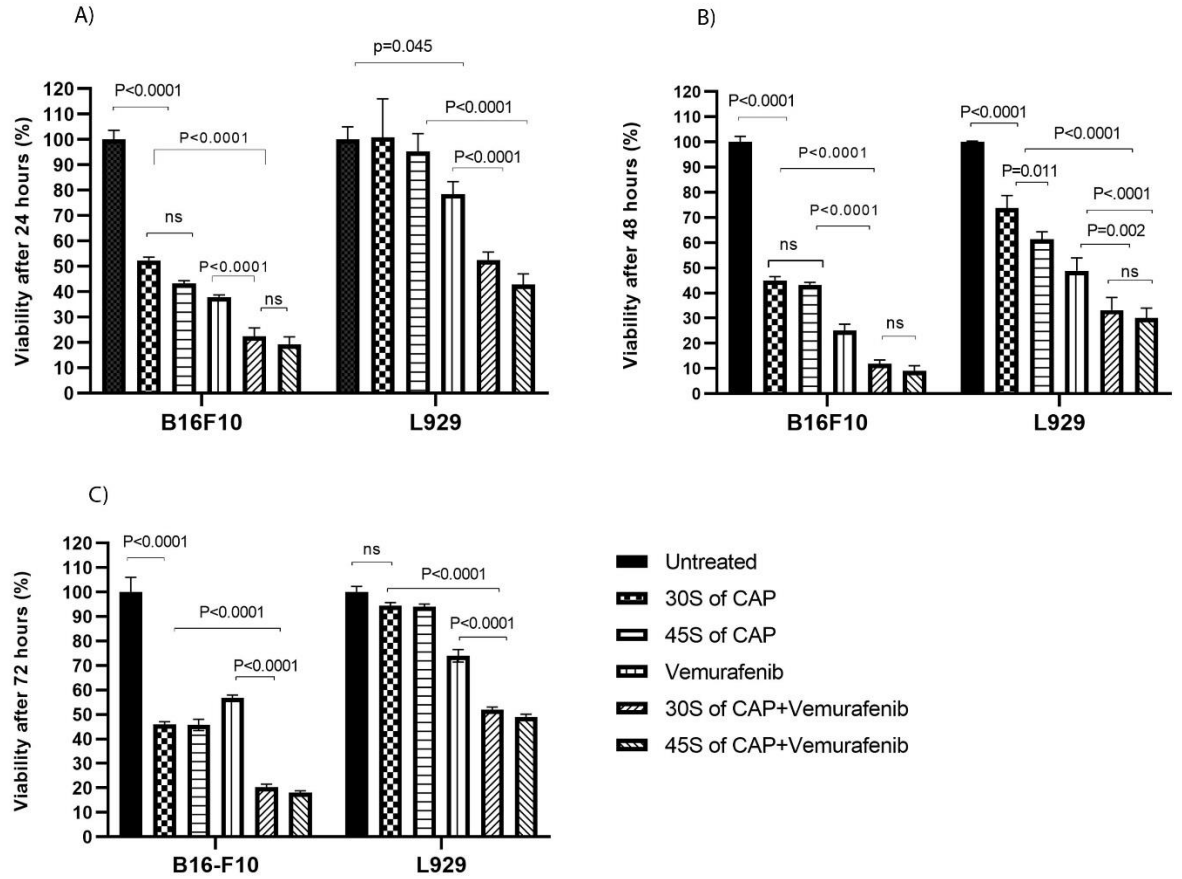

Figure 2. Evaluation of cytotoxic effects of cold atmospheric plasma (CAP), Vemurafenib (VEM, 20 μM), and their combination (CAP+VEM) on B16-F10 melanoma and L929 fibroblast cells at different time points. Cell viability was assessed using the MTT assay following treatment with CAP, VEM, or CAP+VEM (A) After 24 hours, (B) 48 hours, or (C) 72 hours. Data are presented as mean ± SD from three independent experiments. Statistical significance was determined by one-way ANOVA followed by Tukey's post hoc test.

CAP+VEM induces morphological changes in melanoma cells

To evaluate the cytotoxic effects of each treatment on melanoma and normal cells, morphological changes were observed in the cells using inverted phase-contrast microscopy. As seen in Figure 3, the untreated group of B16-F10 cells maintained their typical spindle-shaped morphology, strong adherence, and dense cell population. Treatment with CAP alone resulted in moderate morphological alterations, including cell rounding and reduced confluency, indicating partial cytotoxicity. Exposure to VEM caused mild shrinkage and a slight decrease in cell density. Notably, the CAP+VEM induced substantial morphological damage, characterized by extensive cell detachment, shrinkage, and rounding—features consistent with advanced apoptotic or necrotic processes. In contrast, L929 fibroblast cells showed no significant morphological changes across CAP or VEM conditions. However, CAP+VEM induced moderate changes in L929 cell shape, while maintaining intact membranes and confluency. These findings suggest that the selective cytotoxicity of CAP+VEM is directed toward melanoma cells. These observations support the hypothesis that CAP enhances the cytotoxic effect of VEM selectively in malignant melanoma cells, while sparing normal cells.

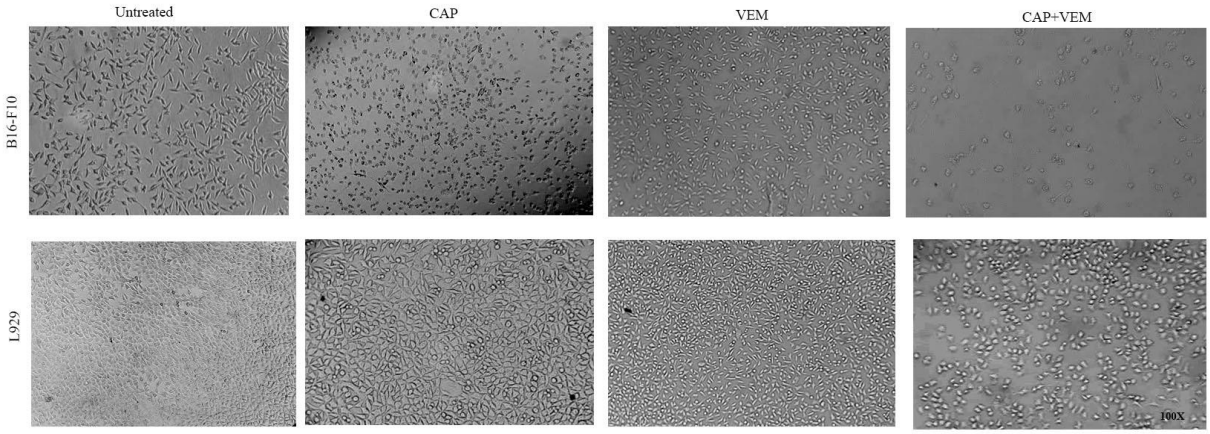

Figure 3. Morphological evaluation of B16-F10 melanoma and L929 fibroblast cells following treatment. Representative phase-contrast microscopy images of B16-F10 (top row) and L929 (bottom row) cells following treatment with cold atmospheric plasma (CAP), Vemurafenib (VEM), or their combination (CAP+VEM) for 24 hours. B16-F10 cells exhibited significant morphological alterations such as cell shrinkage, rounding, and detachment, particularly in the CAP+VEM group, indicative of enhanced cytotoxicity. In contrast, L929 cells retained normal morphology across all treatment conditions, suggesting selective effects of the treatments on melanoma cells. Images were taken at 100× magnification using an inverted phase-contrast microscope.

CAP+VEM amplifies RONS in melanoma cells

Intracellular ROS levels were quantified using DCFH‑DA fluorescence intensity 24 h after treatment (Figure 4A). In B16‑F10 melanoma cells, CAP exposure markedly increased ROS production, with mean fluorescence intensity (MFI) rising from 10.9 in untreated cells to 30.1. Treatment with VEM alone produced a moderate increase (MFI = 23.9), whereas the combined CAP+VEM treatment resulted in the highest ROS generation (MFI = 54). The positive control showed a strong ROS signal (MFI = 78), confirming the sensitivity of the assay. In contrast, pretreatment with the ROS scavenger catalase markedly suppressed ROS production, reducing the signal to 0.23. A similar pattern was observed in L929 normal fibroblasts, although the overall MFI was lower than that observed in melanoma cells. The MFI value increased from 1.14 in untreated cells to 5.85 following CAP exposure, while VEM alone induced a moderate increase (MFI = 2.48). The combined CAP+VEM treatment produced the highest ROS level (MFI = 12.0). The positive control reached an MFI of 23, whereas catalase pretreatment markedly reduced ROS levels to 0.14. These findings indicate that CAP and CAP+VEM treatments

significantly enhance intracellular ROS generation, and the marked suppression by catalase supports the involvement of ROS in the observed cellular responses.

NO production was significantly elevated in both cell lines following CAP treatment (P<0.0001) (Figure 4B). In B16‑F10 cells, CAP increased NO concentration from approximately 25 µM in untreated cells up to ~270 µM, while CAP+VEM further enhanced NO levels to ~230–250 µM, significantly exceeding the VEM group (P<0.0001). VEM monotherapy did not significantly alter NO levels in either cell line. L929 cells also showed an increase in NO following CAP and CAP+VEM (~ 180–200 µM), but the magnitude remained lower than that observed in melanoma cells, indicating a tumor‑selective amplification of RNS generation.

ROS are among the major contributors to lipid peroxidation in cellular membranes. In B16‑F10 melanoma cells, MDA levels increased from ~ 4 µM (untreated) to ~ 14 µM with CAP, and further to ~12–13 µM in the CAP+VEM group. VEM alone caused a smaller but significant increase (~ 8 µM, P<0.0001). In L929 fibroblasts, CAP and CAP+VEM also elevated MDA levels (P<0.0001), but the overall concentrations (~ 3–6 µM) remained markedly lower than those in B16‑F10 cells. These results indicate that lipid peroxidation occurs more robustly in melanoma cells, consistent with their higher susceptibility to RONS‑mediated cytotoxicity.

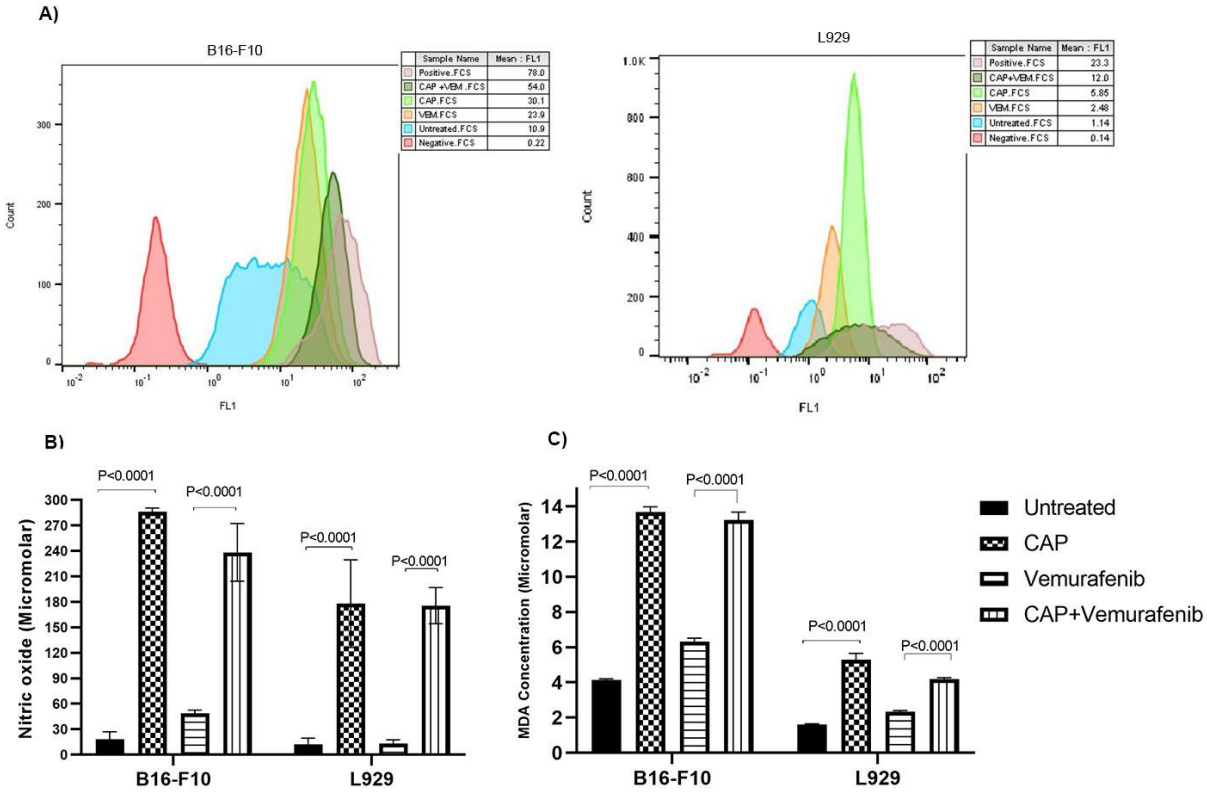

Figure 4. Effect of cold atmospheric plasma (CAP), Vemurafenib (VEM), or their combination (CAP+VEM) treatments on (A) reactive oxygen species (ROS) production, (B) Nitric oxide (NO) production, and (C) lipid peroxidation (MDA) in B16-F10 melanoma and L929 normal murine cell lines after 24 hours. Statistical significance was determined by one-way ANOVA followed by Tukey's post hoc test.

CAP+VEM induces profound cell cycle arrest

The results of flow cytometric assay of the cell cycle demonstrated that treatment with CAP or VEM individually caused modest alterations in cell cycle distribution. This was illustrated by an increase in the G1 phase and a reduction in the S phase population in B16-F10 cells compared to untreated cells. CAP+VEM markedly enhanced

this effect, resulting in a substantial elevation of the G2 fraction relative to single treatments, indicating an amplified induction of apoptosis. Concurrently, a significant decrease in the S phase was observed, suggesting a disruption of normal cell cycle progression. These findings provide early evidence of apoptosis induction by CAP+VEM, as reflected by increased DNA fragmentation and cell cycle arrest in cancerous cells (Figure 5).

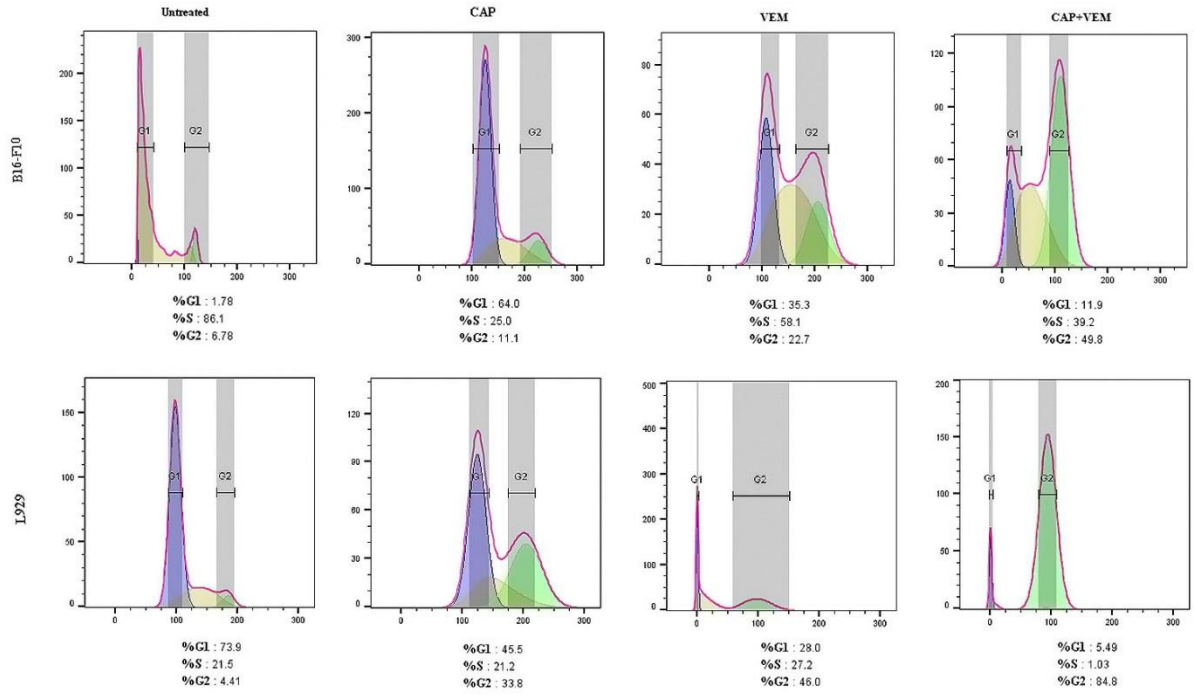

Figure 5. Analysis of cell cycle distribution in B16-F10 melanoma cells following treatment with cold atmospheric plasma (CAP), Vemurafenib (VEM), or their combination (CAP+VEM). Cell cycle profiles were determined by flow cytometric analysis after PI staining. Two cell lines were treated with CAP, VEM, or CAP+VEM for 24 hours. Representative histograms of DNA content are shown, and cell populations in G1, S, and G2/M phases were quantified. Treatment with VEM or CAP alone reduced the S phase population in B16-F10 cells, while CAP+VEM resulted in a marked enhancement of this effect.

CAP+VEM induces apoptosis in a tumor‐selective manner

Apoptotic cell death was evaluated using Annexin V-FITC/PI staining. In B16‐F10 melanoma cells, CAP monotherapy markedly increased the proportion of apoptotic cells (≈42%), indicating a strong induction of programmed cell death compared with the untreated and VEM‐treated groups. VEM alone produced only a minimal rise, remaining close to baseline levels. The CAP+VEM combination resulted in the highest apoptotic response, with approximately 78% of the cell population undergoing apoptosis, demonstrating an enhancement beyond either monotherapy. In contrast, L929 normal fibroblasts exhibited minimal apoptosis across all treatment conditions. CAP, VEM, and CAP+VEM each induced only a slight increase (~6–8%) relative to untreated cells, indicating that apoptosis induction was highly tumor‐selective and preferentially activated in melanoma cells.

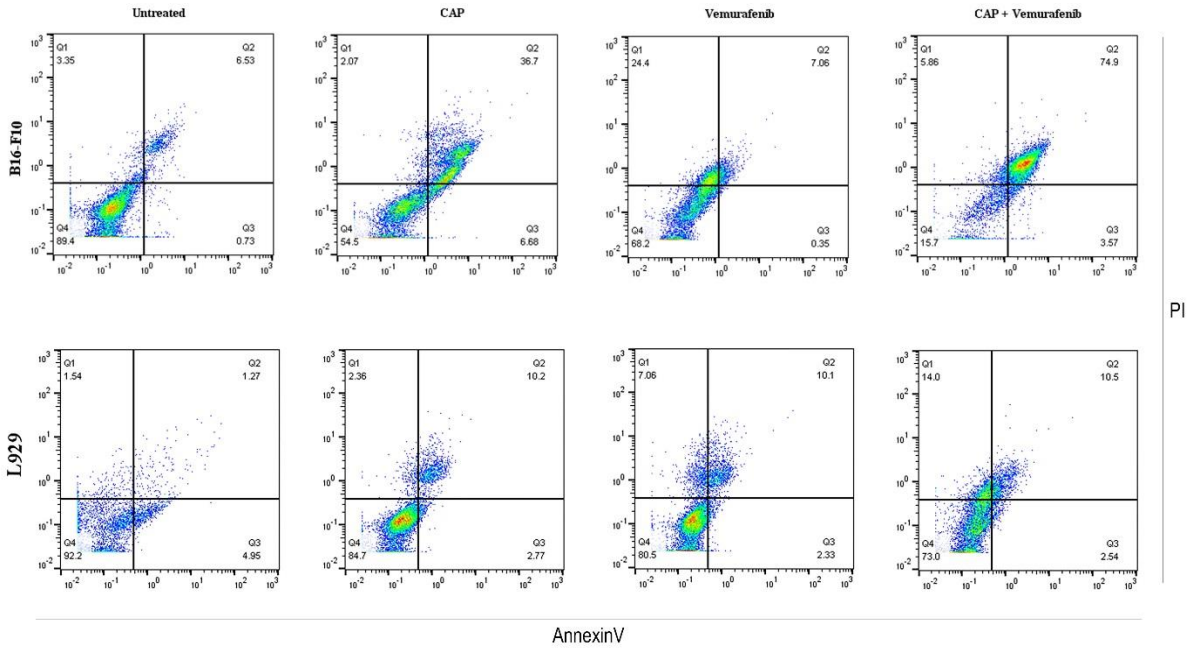

Figure 6. Analysis of apoptosis in the B16-F10 cell line and L929 cells after treatment with cold atmospheric plasma (CAP), Vemurafenib (VEM), and their combination (CAP+VEM) using apoptotic gene expression and annexin V-FITC/PI staining. B16-F10 cells were treated with CAP, VEM, or CAP+VEM for 24 hours. Apoptotic cell death was evaluated using Annexin V-FITC/PI dual staining followed by flow cytometry. Representative dot plots show the distribution of live cells (Annexin V^-/PI^-, lower left), early apoptotic cells (Annexin V^+/PI^-, lower right), late apoptotic cells (Annexin V^+/PI^+, upper right), and necrotic cells (Annexin V^-/PI^+, upper left).

CAP+VEM markedly suppresses melanoma tumor growth

To further evaluate the antitumor efficacy of CAP+VEM *in vivo*, a murine melanoma model was established by the subcutaneous inoculation of B16‑F10 cells into C57BL/6 mice. Treatments were initiated when tumors became palpable. As shown in Figure 7A, tumors in the untreated control group exhibited rapid and progressive growth, reaching volumes of approximately 1400–1500 mm^3 by day 12. In contrast, both CAP and VEM monotherapies significantly suppressed tumor growth compared with the untreated group ($P<0.0001$). CAP‑treated mice showed a marked reduction in tumor progression, with mean tumor volumes remaining below 500 mm^3 at the end of the experiment. Similarly, VEM monotherapy significantly inhibited tumor growth, resulting in mean tumor volumes of approximately 400–450 mm^3 on day 12. Notably, the CAP+VEM treatment produced the greatest antitumor effect, leading to a pronounced and sustained suppression of tumor growth. Tumor volumes in the CAP+VEM group remained below 200 mm^3 throughout the study and were significantly lower than those observed in the untreated group ($P<0.0001$).

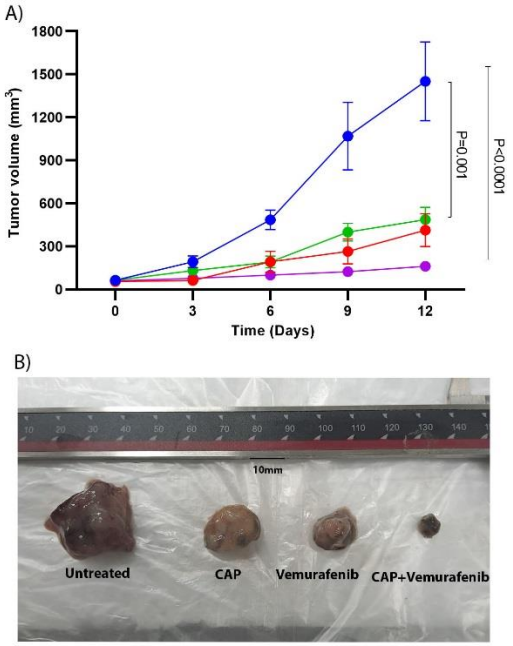

Figure 7. *In vivo* antitumor efficacy of cold atmospheric plasma (CAP), vemurafenib (VEM), and their combination in a murine melanoma model. A) Tumor volume progression in C57BL/6 mice bearing B16-F10 melanoma tumors following the indicated treatments. Both CAP and VEM monotherapies significantly attenuated tumor growth compared with the untreated control group ($P<0.001$), whereas the CAP+VEM combination produced the most pronounced suppression of tumor progression ($P<0.0001$). Data are presented as mean ± SEM (n = 5 per group). B) Representative excised tumors from each treatment group at the end of the study, illustrating the markedly reduced tumor size in CAP+VEM mice.

CAP+VEM modulates apoptosis‐ and autophagy‐related gene expression in melanoma

To assess apoptosis at the transcriptional level, the expression of key apoptotic genes was measured (Figure 8). In B16‐F10 melanoma cells, CAP+VEM markedly upregulated pro‐apoptotic BAX and CASP3, while significantly downregulating anti‐apoptotic BCL‐2 compared with monotherapies. These changes were not observed in L929 fibroblasts, indicating a selective activation of apoptotic pathways in tumor cells. Autophagy‐related markers also showed a tumor‐selective pattern. ATG5 expression increased significantly after all treatments, and was maximally induced by CAP+VEM, whereas L929 cells showed no significant change. LC3 expression followed a similar trend, with only the CAP+VEM treatment producing a significant increase in B16‐F10 cells. LC3 levels remained unchanged in L929 cells under all treatment conditions. Collectively, these findings indicate a preferential transcriptional activation of both apoptosis and autophagy in melanoma cells. Molecular analysis in tumor tissues confirmed the *in vitro* observations. CAP+VEM significantly increased the expression of pro‐apoptotic BAX (≈3‐fold) and CASP3 (≈6–8‐fold), while BCL‐2 showed a non‐significant downward trend. The autophagy‐related marker LC3 was also strongly induced, with an increase of 8–10‐fold elevation. Meanwhile, the ATG5 gene showed a non-significant elevation. These coordinated changes indicate that CAP enhances the apoptotic response to VEM and promotes autophagy‐related transcriptional activation *in vivo*.

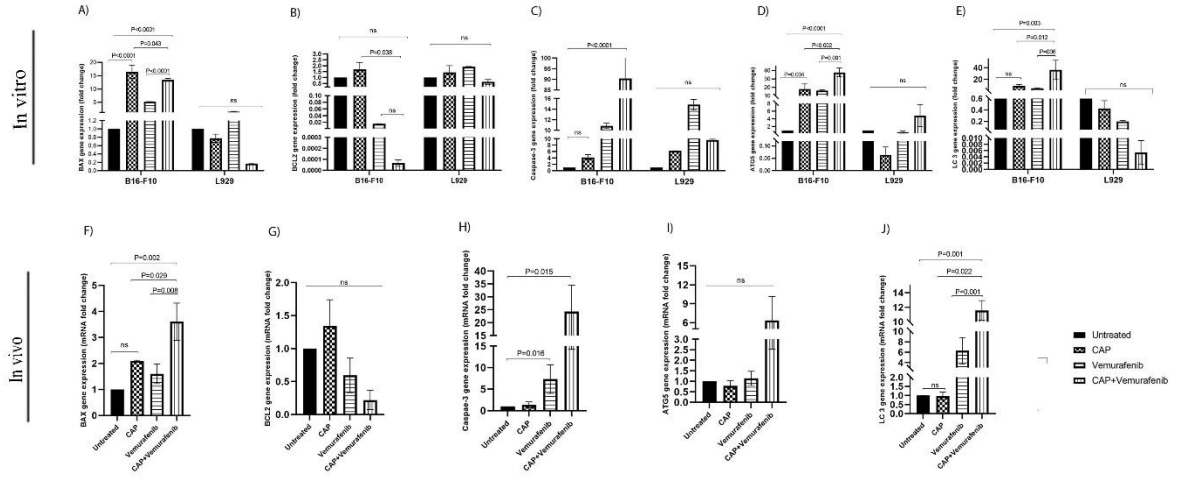

Figure 8. Transcriptional profiling of apoptosis- and autophagy-related genes in melanoma cells and tumor tissues. (A–E) Quantitative PCR (qPCR) analysis of mRNA expression levels for pro-apoptotic (BAX, CASP3), anti-apoptotic (BCL2), and autophagy-related markers (ATG5, LC3) in B16-F10 melanoma cells and L929 normal fibroblasts 24 h post-treatment. Selective transcriptional activation is observed in melanoma cells compared to normal fibroblasts. (F–J) Relative mRNA expression of the corresponding genes in malignant melanoma tumor tissues harvested from the *in vivo* model, demonstrating the molecular impact of CAP+VEM within the tumor microenvironment. Data are presented as mean ± SEM of at least three independent experiments. Statistical significance was determined by one-way ANOVA followed by LSD post hoc test. Exact P-values are indicated above the comparison brackets; ns denotes non-significant differences ($P > 0.05$). CAP: Cold Atmospheric Plasma; VEM: Vemurafenib.

Discussion

This study demonstrates that CAP enhances the anti-cancer effects of VEM in melanoma models *in vitro* and *in vivo*. These effects appear to be mediated by the overproduction of RONS, which are well-established mediators of redox stress and apoptosis in cancer therapy. Both CAP and VEM induce ROS generation.[10,12,44,45] Thus, the combination therapy of the two approaches may amplify an oxidative environment. Several studies have previously reported that elevated RONS levels disrupt redox homeostasis, leading to oxidative modifications in DNA, proteins, and lipids, eventually promoting cell death. [46-50] In line with these findings, our results revealed a significant increase in ROS generation, NO formation, and lipid peroxidation in the CAP+VEM treated melanoma cells. This suggests that membrane destabilization is a possible early step in apoptosis induction. The role of oxidative stress in triggering programmed cell death was further supported by cell cycle analysis, which indicated an arrest in the S phase. These data align with previous reports indicating that ROS generation and DNA damage can activate checkpoint responses, arresting cells in the S phase of the cycle to facilitate apoptosis.[51,52]

Flow cytometry analysis using Annexin V-FITC/PI staining revealed that CAP and VEM alone induced approximately 42% and 7% apoptosis, respectively, in tumor cells, whereas the CAP+VEM combination dramatically increased apoptotic rates. This finding is consistent with previous observations in other cancer models treated with CAP-based combination therapies.[35,53,54] Molecular profiling suggests transcriptional upregulation of BAX and CASP3, along with downregulation of BCL-2 genes. These gene level findings propose the potential involvement of the intrinsic mitochondrial apoptotic pathway. Interestingly, our study also observed a significant increase in the autophagy-related genes LC3 and ATG5, in the CAP+VEM group. While autophagy is classically considered a survival mechanism under metabolic stress, its excessive or dysregulated activation has been increasingly recognized as a pro-death pathway under sustained oxidative pressure.[55,56] The combination treatment in our study led to a robust autophagic gene response, represent a possible shift toward autophagic cell death. However, because autophagic flux was not directly assessed, it remains unclear whether the observed

changes reflect activation of autophagy or a blockade of autophagic degradation. Further studies using established autophagy‐flux assays will be required to clarify the precise role of autophagy in this context.

Importantly, our *in vivo* findings further validated the enhanced therapeutic efficacy of the combination therapy. In the murine melanoma model, CAP or VEM alone significantly reduced tumor growth compared with the untreated control group, but the co-treatment produced the most pronounced suppression of tumor progression. Tumor volumes were markedly smaller in the CAP+VEM group, demonstrating a strong inhibitory effect on melanoma development. These results indicate that the oxidative and molecular alterations observed *in vitro* translate into measurable antitumor activity in a physiological environment. Furthermore, molecular analysis of tumor tissues revealed increased expression of the genes BAX and CASP3, while BCL‐2 expression showed a decreasing trend *in vivo*, generally consistent with the patterns observed in cultured cells. In addition, the concurrent upregulation of LC3 and ATG5 in tumor tissues suggests the involvement of autophagy‐related pathways in the treatment response.

Furthermore, these findings should be interpreted within the broader context of melanoma biology and targeted therapy. While VEM is highly effective for BRAF-mutated melanomas, acquired resistance and dose-limiting toxicities remain major clinical hurdles. Although the present study utilized VEM-sensitive melanoma cells and did not directly investigate VEM-resistant models, our prelaminar data indicate that CAP could serve as a promising adjunctive strategy to enhance VEM efficacy in melanoma cells, potentially exploiting their unique vulnerability to redox stress. Future studies are required to determine whether this combination can overcome acquired resistance. Despite the promising outcomes, several important limitations should be acknowledged. Although our data suggest that CAP enhances the antitumor activity of VEM, all experiments were performed using the VEM‐sensitive B16‐F10 mouse melanoma cell line. Therefore, the present findings cannot be directly extrapolated to VEM‐resistant melanoma, and we cannot definitely conclude that CAP is capable of overcoming clinically relevant resistance mechanisms. Future studies incorporating established VEM‐resistant cell lines, long‐term drug‐pressure models, or patient‐derived melanoma cells will be essential to determine whether CAP can modulate known resistance pathways such as MAPK reactivation or PI3K/AKT upregulation. In addition, although the molecular data revealed apoptosis‐ and autophagy‐associated responses both *in vitro* and *in vivo*, deeper mechanistic analyses—including evaluation of BRAF downstream signaling, ERK phosphorylation dynamics, and CAP‐induced alterations in drug uptake—were beyond the scope of the present study. Additionally, validation of apoptotic markers at the protein‐level, such as cleaved caspase‐3 or PARP, was not performed. Therefore, although our findings support activation of apoptotic pathways, further protein‐based analyses will be required to fully confirm the molecular mechanisms underlying CAP‐ and VEM‐induced apoptosis. Moreover, although increased expression of LC3 and ATG5 suggests the involvement of autophagy‐related pathways in the cellular response to CAP and VEM, the functional role of autophagy in this context remains unclear. Autophagy can act either as a cytoprotective mechanism that enables tumor cells to adapt to oxidative stress or as a cell‐death–associated process under conditions of excessive cellular damage. Because functional inhibition and autophagic flux analyses were not performed in the present study, we cannot definitively distinguish between pro‐survival and pro‐death autophagy. Future investigations using pharmacological autophagy inhibitors and genetic

modulation of key autophagy regulators will be necessary to clarify the precise role of autophagy in CAP‐ and VEM‐treated melanoma cells.

Conclusion

Collectively, our findings indicate that the CAP+VEM combination induces an enhanced antitumor response in melanoma cells. This effect may be mediated through a multifactorial mechanism involving redox-mediated membrane damage, disruption of cell cycle progression, and activation of both apoptosis and autophagy. Notably, these effects were less pronounced in normal L929 cells, suggesting a degree of selectivity for this approach. These findings were corroborated *in vivo*, where CAP+VEM reduced tumor growth compared with either monotherapy. Melanoma gene expression in vitro and *in vivo* showed increased levels of BAX and CASP3, decreased BCL-2, and upregulation of LC3 and ATG5. Although this study was performed in a VEM‐sensitive melanoma model, these results highlight the potential of CAP as an adjuvant strategy to enhance targeted therapy. Further investigations using VEM‐resistant melanoma models are required to clarify its broader therapeutic applicability.

Authors Contribution

Conceptualization: Zahra Yazdani, Alireza Rafiei

Methodology: Zahra Yazdani, Farshad Sohbatzadeh, Monireh Golpour, Sadegh Fattahi, Alireza Rafiei

Validation: Zahra Yazdani, Alireza Rafiei

Investigation: Zahra Yazdani, Farshad Sohbatzadeh, Saeid Abediankenari, Monireh Golpour, Alireza Rafiei

Data Curation: Zahra Yazdani

Project Administration: Alireza Rafiei

Funding Acquisition: Alireza Rafiei

Visualization: Zahra Yazdani, Farshad Sohbatzadeh, Saeid Abediankenari, Monireh Golpour, Alireza Rafiei

Supervision: Alireza Rafiei

Writing - Original Draft: Zahra Yazdani, Alireza Rafiei

Writing - Review & Editing: Zahra Yazdani, Saeid Abediankenari, , Alireza Rafiei

Acknowledgements

During the preparation of this manuscript, the authors used ChatGPT (OpenAI, San Francisco, CA, USA) to assist with language editing and to improve the clarity and readability of the text. The tool was also used to help draft the schematic illustration presented in graphical abstract, based on the authors' conceptual design and scientific interpretation. The artificial intelligence tool was not used to generate scientific data, perform data analysis, or independently interpret the results. All experimental data, analyses, interpretations, and conclusions were developed and verified by the authors, who take full responsibility for the accuracy and integrity of the work.

Ethics Approval and Consent to Participate

The protocol of this study approved by the Research Ethics committee of Mazandaran University of Medical Science IR.MAZUMS.AEC.1402.079.

Availability of data and materials

The data that support the findings of this study are available from the corresponding author upon reasonable request.

Competing interests

The authors declare that they have no competing interests.

Funding

This research was funded by Research and Technology Deputy of Mazandaran University of Medical Sciences., grant number 15127, and National Institute for Medical Research Development (NIMAD), grant number 4031031.

References

1. Wang Y, Mang X, Li D, Chen Y, Cai Z, Tan F. Piezoeletric cold atmospheric plasma induces apoptosis and autophagy in human hepatocellular carcinoma cells through blocking glycolysis and AKT/mTOR/HIF-1α pathway. *Free Radic Biol Med* 2023;208:134-52. DOI: 10.1016/j.freeradbiomed.2023.07.036
2. Roky AH, Islam MM, Ahasan AMF, Mostaq MS, Mahmud MZ, Amin MN, et al. Overview of skin cancer types and prevalence rates across continents. *Cancer Pathog Ther* 2025;3(02):89-100. DOI: 10.1016/j.cpt.2024.08.002
3. Sung H, Ferlay J, Siegel RL, Laversanne M, Soerjomataram I, Jemal A, et al. Global cancer statistics 2020: GLOBOCAN estimates of incidence and mortality worldwide for 36 cancers in 185 countries. *CA Cancer J Clin* 2021;71(3):209-49. DOI: 10.3322/caac.21660
4. Soengas MS, Lowe SW. Apoptosis and melanoma chemoresistance. *Oncogene* 2003;22(20):3138-51. DOI: 10.1038/sj.onc.1206454
5. Rafiei A, Sohbatzadeh F, Hadavi S, Bekeschus S, Alimohammadi M, Valadan R. Inhibition of murine melanoma tumor growth in vitro and in vivo using an argon-based plasma jet. *Clinical Plasma Medicine* 2020;19:100102 DOI: 10.1016/j.cpme.2020.100102
6. Luke JJ, Hodi FS. Vemurafenib and BRAF inhibition: a new class of treatment for metastatic melanoma. *Clin Cancer Res* 2012;18(1):9-14. DOI: 10.1158/1078-0432.CCR-11-2197
7. Sharma A, Shah SR, Illum H, Dowell J. Vemurafenib: targeted inhibition of mutated BRAF for treatment of advanced melanoma and its potential in other malignancies. *Drugs* 2012;72(17):2207-22. DOI: 10.2165/11640870-000000000-00000
8. Chanda M, Cohen MS. Advances in the discovery and development of melanoma drug therapies. *Expert Opin Drug Discov* 2021;16(11):1319-47. DOI: 10.1080/17460441.2021.1942834
9. Teppo H-R, Soini Y, Karihtala P. Reactive oxygen species-mediated mechanisms of action of targeted cancer therapy. *Oxid Med Cell Longev* 2017;2017(1):1485283. DOI: 10.1155/2017/1485283
10. Bauer D, Werth F, Nguyen HA, Kiecker F, Eberle J. Critical role of reactive oxygen species (ROS) for synergistic enhancement of apoptosis by vemurafenib and the potassium channel inhibitor TRAM-34 in melanoma cells. *Cell Death Dis* 2017;8(2):e2594-e. DOI: 10.1038/cddis.2017.6
11. Wang L, Otkur W, Wang A, Wang W, Lyu Y, Fang L, et al. Norcantharidin overcomes vemurafenib resistance in melanoma by inhibiting pentose phosphate pathway and lipogenesis via downregulating the mTOR pathway. *Front Pharmacol* 2022;13:906043. DOI: 10.3389/fphar.2022.906043
12. Morlière P, Boscá F, Silva A, Teixeira A, Galmiche A, Mazière J, et al. A molecular insight into the phototoxic reactions observed with vemurafenib, a first-line drug against metastatic melanoma. *Photochem Photobiol Sci* 2015;14(11):2119-27. DOI: 10.1039/c5pp00231a

13. Martin S, Dudek-Perić A, Maes H, Garg A, Gabrysiak M, Demirsoy S, et al. Concurrent MEK and autophagy inhibition is required to restore cell death associated danger-signalling in Vemurafenib-resistant melanoma cells. *Biochem Pharmacol* 2015;93(3):290-304. DOI: 10.1016/j.bcp.2014.12.003

14. Das Thakur M, Salangsang F, Landman AS, Sellers WR, Pryer NK, Levesque MP, et al. Modelling vemurafenib resistance in melanoma reveals a strategy to forestall drug resistance. *Nature* 2013;494(7436):251-5. DOI: 10.1038/nature11814

15. Romano E, Pradervand S, Paillusson A, Weber J, Harshman K, Muehlethaler K, et al. Identification of multiple mechanisms of resistance to vemurafenib in a patient with BRAFV600E-mutated cutaneous melanoma successfully rechallenged after progression. *Clin Cancer Res* 2013;19(20):5749-57. DOI: 10.1158/1078-0432.CCR-13-0661

16. Arslanbaeva LR, Santoro MM. Adaptive redox homeostasis in cutaneous melanoma. *Redox Biol* 2020;37:101753. DOI: 10.1016/j.redox.2020.101753

17. Alimohammadi M, Golpour M, Sohbatzadeh F, Hadavi S, Bekeschus S, Niaki HA, et al. Cold atmospheric plasma is a potent tool to improve chemotherapy in melanoma in vitro and in vivo. *Biomolecules* 2020;10(7):1011. DOI: 10.3390/biom10071011

18. Jawaid P, Rehman MU, Zhao QL, Takeda K, Ishikawa K, Hori M, et al. Helium-based cold atmospheric plasma-induced reactive oxygen species-mediated apoptotic pathway attenuated by platinum nanoparticles. *J Cell Mol Med* 2016;20(9):1737-48. DOI: 10.1111/jcmm.12880

19. Yazdani Z, Mehrabanjoubani P, Biparva P, Rafiei A. Cytotoxicity effect of cold atmospheric plasma on melanoma (B16-F10), breast (MCF-7) and lung (A549) cancer cell lines compared with normal cells. *Journal of Mazandaran University of Medical Sciences* 2020;30(187):38-48.

20. Faramarzi F, Zafari P, Alimohammadi M, Moonesi M, Rafiei A, Bekeschus S. Cold physical plasma in cancer therapy: mechanisms, signaling, and immunity. *Oxid Med Cell Longev* 2021;2021(1):9916796. DOI: 10.1155/2021/9916796

21. Golpour M, Sohbatzadeh F, Alimohammadi M, Yazdani Z, Fattahi S, Zaboli E, et al. Increased Expression of ITGB 3 in CLL Patient leukemia Cells by Exposure to Cold Physical Plasma and Plasma-treated Medium. *Int J Mol Cell Med* 2024;13(3):248. DOI: 10.22088/IJMCM.BUMS.13.3.248

22. Golpour M, Asgarian-Omran H, Akhavan-Niaki H, Alimohammadi M, Alizadeh-Forutan M, Sohbatzadeh F, et al. Cold plasma treatment of patient-derived chronic lymphocytic B-cell leukemia enhances cytotoxic T-cell proliferation. *Plasma Processes and Polymers* 2024;21(9):2400008. DOI: 0.1002/ppap.202400008

23. Mahdikia H, Saadati F, Freund E, Gaipl US, Majidzadeh-a K, Shokri B, et al. Gas plasma irradiation of breast cancers promotes immunogenicity, tumor reduction, and an abscopal effect in vivo. *Oncoimmunology* 2021;10(1):1859731. DOI: 10.1080/2162402X.2020.1859731

24. Bekeschus S, Saadati F, Emmert S. The potential of gas plasma technology for targeting breast cancer. *Clin Transl Med* 2022;12(8):e1022. DOI: 10.1002/ctm2.1022

25. Mahdikia H, Shokri B, Majidzadeh-A K. The feasibility study of plasma-activated water as a physical therapy to induce apoptosis in melanoma cancer cells in-vitro. *Iran J Pharm Res* 2021;20(3):337. DOI: 10.22037/ijpr.2021.114493.14882

26. Hasse S, Meder T, Freund E, von Woedtke T, Bekeschus S. Plasma treatment limits human melanoma spheroid growth and metastasis independent of the ambient gas composition. *Cancers* 2020;12(9):2570. DOI: 10.3390/cancers12092570

27. Bekeschus S, Ispirjan M, Freund E, Kinnen F, Moritz J, Saadati F, et al. Gas plasma exposure of glioblastoma is cytotoxic and immunomodulatory in patient-derived GBM tissue. *Cancers* 2022;14(3):813. DOI: 10.3390/cancers14030813

28. Soni V, Adhikari M, Lin L, Sherman JH, Keidar M. Theranostic potential of adaptive cold atmospheric plasma with temozolomide to checkmate glioblastoma: An in vitro study. *Cancers* 2022;14(13):3116. DOI: 10.3390/cancers14133116

29. Yan D, Sherman JH, Keidar M. Cold atmospheric plasma, a novel promising anti-cancer treatment modality. *Oncotarget* 2016;8(9):15977. DOI: 10.18632/oncotarget.13304

30. Graves DB. The emerging role of reactive oxygen and nitrogen species in redox biology and some implications for plasma applications to medicine and biology. *Journal of Physics D: Applied Physics* 2012;45(26):263001.

31. Golpour M, Alimohammadi M, Sohbatzadeh F, Fattahi S, Bekeschus S, Rafiei A. Cold atmospheric pressure plasma treatment combined with starvation increases autophagy and apoptosis in melanoma in vitro and in vivo. *Exp Dermatol* 2022;31(7):1016-28. DOI: 10.1111/exd.14544

32. Jalili A, Irani S, Mirfakhraie R. Combination of cold atmospheric plasma and iron nanoparticles in breast cancer: Gene expression and apoptosis study. *Onco Targets Ther* 2016:5911-7. DOI: 10.2147/OTT.S95644

33. Zhu W, Lee S-J, Castro NJ, Yan D, Keidar M, Zhang LG. Synergistic effect of cold atmospheric plasma and drug loaded core-shell nanoparticles on inhibiting breast cancer cell growth. *Sci Rep* 2016;6(1):21974. DOI: 10.1038/srep21974

34. Adhikari M, Adhikari B, Ghimire B, Baboota S, Choi EH. Cold atmospheric plasma and silymarin nanoemulsion activate autophagy in human melanoma cells. *Int J Mol Sci* 2020;21(6):1939. DOI: 10.3390/ijms21061939

35. Adhikari M, Kaushik N, Ghimire B, Adhikari B, Baboota S, Al-Khedhairy AA, et al. Cold atmospheric plasma and silymarin nanoemulsion synergistically inhibits human melanoma tumorigenesis via targeting HGF/c-MET downstream pathway. *Cell Commun Signal* 2019;17(1):52. DOI: 10.1186/s12964-019-0360-4

36. Cossarizza A, Ferraresi R, Troiano L, Roat E, Gibellini L, Bertoncelli L, et al. Simultaneous analysis of reactive oxygen species and reduced glutathione content in living cells by polychromatic flow cytometry. *Nat Protoc* 2009;4(12):1790-7. DOI: 10.1038/nprot.2009.189

37. Park J, Jang Y-S, Choi J-H, Ryu M, Kim G-C, Byun J-H, et al. Anticancer efficacy of nonthermal plasma therapy combined with PD-L1 antibody conjugated gold nanoparticles on oral squamous cell carcinoma. *Applied Sciences* 2021;11(10):4559.

38. Yazdani Z, Pasandi MS, Golpour M, Eslami M, Rafiei A. Effect of cold atmospheric plasma on changing of biomolecular structures involved in apoptosis pathways of melanoma cancer. *Skin Res Technol* 2024;30(1):e13544. DOI: 10.1111/srt.13544

39. Mikula H, Stapleton S, Kohler RH, Vinegoni C, Weissleder R. Design and development of fluorescent vemurafenib analogs for in vivo imaging. *Theranostics* 2017;7(5):1257. DOI: 10.7150/thno.18238

40. Van Meerloo J, Kaspers GJ, Cloos J. Cell sensitivity assays: the MTT assay. Cancer cell culture: methods and protocols: Springer; 2011. p. 237-45. DOI: 10.1007/978-1-61779-080-5_20

41. Miranda KM, Espey MG, Wink DA. A rapid, simple spectrophotometric method for simultaneous detection of nitrate and nitrite. *Nitric oxide* 2001;5(1):62-71. DOI: 10.1006/niox.2000.0319

42. Riccardi C, Nicoletti I. Analysis of apoptosis by propidium iodide staining and flow cytometry. *Nat Protoc* 2006;1(3):1458-61. DOI: 10.1038/nprot.2006.238

43. Fattahi S, Amirbozorgi G, Lotfi M, Amini Navaei B, Kavoosian S, Asouri M, et al. Development of a universal taqman probe for mRNA gene expression analysis. *Iranian Journal of Science and Technology, Transactions A: Science* 2018;42(2):363-70. DOI: 10.1007/s40995-017-0173-5

44. Graves DB. Reactive species from cold atmospheric plasma: Implications for cancer therapy. *Plasma Processes and Polymers* 2014;11(12):1120-7. DOI: 10.1002/ppap.201400068

45. Mitra S, Nguyen LN, Akter M, Park G, Choi EH, Kaushik NK. Impact of ROS generated by chemical, physical, and plasma techniques on cancer attenuation. *Cancers* 2019;11(7):1030. DOI: 10.3390/cancers11071030

46. Simon H-U, Haj-Yehia A, Levi-Schaffer F. Role of reactive oxygen species (ROS) in apoptosis induction. *Apoptosis* 2000;5(5):415-8. DOI: 10.1023/a:1009616228304

47. Zhao Y, Ye X, Xiong Z, Ihsan A, Ares I, Martínez M, et al. Cancer metabolism: the role of ROS in DNA damage and induction of apoptosis in cancer cells. *Metabolites* 2023;13(7):796. DOI: 10.3390/metabo13070796

48. Matés JM, Sánchez-Jiménez FM. Role of reactive oxygen species in apoptosis: implications for cancer therapy. *Int J Biochem Cell Biol* 2000;32(2):157-70. DOI: 10.1016/s1357-2725(99)00088-6

49. Galluzzi L, Vitale I, Aaronson SA, Abrams JM, Adam D, Agostinis P, et al. Molecular mechanisms of cell death: recommendations of the Nomenclature Committee on Cell Death 2018. *Cell Death Differ* 2018;25(3):486-541. DOI: 10.1038/s41418-017-0012-4

50. Girard P-M, Arbabian A, Fleury M, Bauville G, Puech V, Dutreix M, et al. Synergistic effect of H2O2 and NO2 in cell death induced by cold atmospheric He plasma. *Sci Rep* 2016;6(1):29098. DOI: 10.1038/srep29098

51. Sadiq IZ. Free radicals and oxidative stress: Signaling mechanisms, redox basis for human diseases, and cell cycle regulation. *Curr Mol Med* 2023;23(1):13-35. DOI: 10.2174/1566524022666211222161637

52. Fairus AM, Choudhary B, Hosahalli S, Kavitha N, Shatrah O. Dihydroorotate dehydrogenase (DHODH) inhibitors affect ATP depletion, endogenous ROS and mediate S-phase arrest in breast cancer cells. *Biochimie* 2017;135:154-63. DOI: 10.1016/j.biochi.2017.02.003

53. Yazdani Z, Mehrabanjoubani P, Rafiei A, Biparva P, Kardan M. Combined effect of cold atmospheric plasma and curcumin in melanoma cancer. *Biomed Res Int* 2021;2021(1):1969863. DOI: 10.1155/2021/1969863

54. Yan C, Zhao L, Zhang X, Chu Z, Zhou T, Zhang Y, et al. Cold atmospheric plasma sensitizes melanoma cells to targeted therapy agents in vitro. *J Biophotonics* 2024;17(3):e202300356. DOI: 10.1002/jbio.202300356

55. Liu S, Yao S, Yang H, Liu S, Wang Y. Autophagy: Regulator of cell death. *Cell Death Dis* 2023;14(10):648. DOI: 10.1038/s41419-023-06154-8

56. Das S, Shukla N, Singh SS, Kushwaha S, Shrivastava R. Mechanism of interaction between autophagy and apoptosis in cancer. *Apoptosis* 2021;26(9):512-33. DOI: 10.1007/s10495-021-01687-9